CAN UNRESOLVED POINT SOURCES PRODUCE THE DIFFUSE X-RAY EMISSION FROM THE GALACTIC CENTER?

Michael P. Muno
Hubble Fellow; Department of Physics and Astronomy, University of California,Los Angeles, CA 90095
mmuno@astro.ucla.edu

1. INTRODUCTION

The diffuse X-ray emission observed from the Galactic center is an inward extension of emission observed throughout the Galactic plane. However, despite two decades of study, the origin of the emission is still uncertain. The major problem in understanding this diffuse Galactic background is the presence of emission lines emission from He-like and H-like Fe, which are rarely associated with any of the processes that are known to heat the interstellar medium (e.g., Kaneda et al. 1997). Therefore, it has been proposed that this hard diffuse emission is produced by unresolved point sources. Unfortunately, unlike the cosmic X-ray background, the Galactic background has yet to be resolved unambiguously into discrete components.

Several observational clues suggest that the emission is truly diffuse. For instance, the deepest *Chandra* observations of the Galactic plane find that point sources brighter than 3×10^{-15} erg cm^{-2} s^{-1} contribute only 10% to the total diffuse Galactic ridge emission (Ebisawa et al. 2001). Likewise, *ASCA* observations of the Galactic plane reveal degree-scale variations in the intensity of the diffuse emission, which could only be produced by random variations in the numbers of point sources if they have intensities of $\approx 2 \times 10^{-13}$ erg cm^{-2} s^{-1} (Yamauchi et al. 1996). This apparently leaves no flux range over which point sources could account for all of the properties of the diffuse emission.

Nonetheless, the debate is not over. The variations in the intensity of the diffuse emission could be produced by any of several classes of extended X-ray features have been discovered recently, including hot supernova remnants without radio counterparts (Bamba et al. 2003), magnetic filaments (Sakano et al. 2003; Lu, Wang, & Lang 2003), and X-ray reflection nebulae (Sunyaev, Markevitch, & Pavlinsky 1993; Murakami et al. 2000; Yusef-Zadeh, Law, & Wardle 2002). We may also have identified the actual point sources that comprise the apparently diffuse emission. *Chandra* observations of the Galactic center reveal that the faint stellar X-ray sources there have spectra that are remarkably similar to that of the hard component of the diffuse emission (Wang et al. 2002). Moreover, the $\log(N) - \log(S)$ distribution of resolved point sources within 20 pc of Sgr A* is so steep that the flux from unresolved point sources could explain all of the diffuse emission if the distribution extends down to only $\sim 10^{-16}$ erg cm^{-2} s^{-1} (Muno et al. 2003a). Therefore, it still seems plausible that point sources produce the hard background emission observed throughout the Galactic ridge.

The perfect opportunity to examine this question in more detail was recently presented to us in the form of a 626 ks *Chandra* exposure of the 17′ by 17′ field around Sgr A*. Therefore, in this article, we compare the spectra of the point sources and diffuse emission in that field in order to place an upper limit on the fraction of the diffuse emission that is likely to be produced by unresolved point sources.

2. OBSERVATIONS

Twelve separate pointings toward the inner 20 pc of the Galaxy have been carried out in order to monitor Sgr A* (see Table 2 in Muno et al. 2003) using the Advanced CCD Imaging Spectrometer imaging array (ACIS-I) aboard the *Chandra X-ray Observatory* (Weisskopf et al. 2002).The ACIS-I is a set of four 1024-by-1024 pixel CCDs, covering a field of view of 17′ by 17′. When placed on-axis at the focal plane of the grazing-incidence X-ray mirrors, the imaging resolution is determined primarily by the pixel size of the CCDs, 0.″492. The CCDs also measure the energies of incident photons, with a resolution of 50–300 eV (depending on photon energy and distance from the readout node) within a calibrated energy band of 0.5–8 keV.

The raw event lists from each observation were processed and combined as described in Muno et al. (2003a). The resulting raw image is displayed in Figure 1, while a smoothed three-color image is presented in Figure 2. We identified 2353 point sources in this image using a wavelet-decomposition algorithm (`wavdetect`), and extracted spectra for groups of sources based on their intensity and spectrum. Next, we isolated the diffuse emission, using the mask illustrated by the circles in Figure 1 to remove the point sources. Figures 3 and 4 display the resulting images in the 2–4 keV and 4–8 keV bands, respectively. The spectra of the diffuse emission were extracted from the regions indicated in these figures. Representative spectra of the diffuse emission and point sources are displayed in Figure 5.

We modeled the spectra of the point sources and the diffuse emission using a standard least-χ^2 fitting package (`XSPEC`). We assumed the diffuse emission was produced by two thermal plasma components (the model `vapec`) and a Gaussian line to account for low-ionization Fe K-α emission at 6.4 keV. We allowed the abundances of Si, S, Ar, Ca, and Fe in the plasma model to vary independently, although we applied the same values to each component. We assumed that each plasma was absorbed by a different column of gas, which was modeled as (1) a uniform absorber that applied to the entire image plus (2) a partial-covering absorber that applied to a fraction f of the image. We will report the detailed results of the modeling in up-coming publications, so we only summarize them below.

2.1. *Diffuse Emission*

For the diffuse emission, we found that the lines of Si, S, Ar, and Ca constrain the low-temperature plasma to have $kT_1 \approx 0.8$ keV, while the continuum and Fe emission constrained the hotter component to have $kT_2 \approx 8$ keV. The fluxes from each continuum component in each region are listed in Table 1.

The hard component of the diffuse emission is most important to the current study, because its spectrum closely resembles that of the point sources in Figure 5. The surface brightness of the hard component varies by a factor of two across the image, from 1.5×10^{-13} erg cm^{-2} s^{-1} arcmin^{-2} in the darkest region to 2.6×10^{-13} erg cm^{-2} s^{-1} arcmin^{-2} in the Northeast (Figure 4). The inferred temperature of the plasma varies between 6–9 keV, because there are significant variations in the equivalent widths and flux ratios of the He-like and H-like iron lines.

The properties of the soft component represent a bit of a tangent. Its surface brightness is highest by far in the Northeast region, where the hard emission is also most intense (see Figure 3). This suggests that production mechanisms for the two plasma components are related.

2.2. *Point Sources*

As is clear from Figure 5, the point sources on average have a much harder spectrum than does the diffuse emission. Under the two-kT model used above, we find that the soft component of the plasma model is heavily absorbed in the point sources, so that it contributes only 3% of the total observed 2–8 keV flux. The hot plasma component, with a temperature of 9 keV, contributes the remainder of the flux. It is this hot component that produces the He-like and H-like iron lines that appear so similar to those in the diffuse emission (compare Wang et al. 2002).

In order to establish a fiducial spectrum for the unresolved point sources, examined the spectra of the resolved sources as a function of their intensity. We selected only those sources which were not detected below 1.5 keV, as these are most likely to lie near the Galactic center. We found that the averaged spectra varied very little. The only significant trends were that as the point sources considered became fainter (1) that He-like Fe emission at 6.7 and 6.9 keV increased in intensity, while (2) the low-ionization Fe emission at 6.4 keV decreased in intensity. Therefore, for our fiducial point-source spectrum we used the faintest sources, those with fewer than 80 net counts.

We also note that, in contrast to the diffuse emission, the flux from resolved point sources in nearly constant at any given offset from Sgr A*. The fluxes from resolved point sources in each region are listed in Table 1.

3. RESULTS

We determined an upper limit to the amount of flux that unresolved point sources can contribute to the diffuse emission by adding a spectral component representing the faintest resolved point sources to our model for the diffuse emission. The unresolved point sources were assumed to have a fixed spectral shape identical to that of the resolved sources with fewer than 80 net counts. The normalization of the point-source component was then stepped over a range of values, while the the temperatures, elemental abundances, and normalizations of the model for the diffuse emission were allowed to vary to minimize χ^2 for each normalization. We then found the largest value of the point-source normalization for which we obtained a χ^2 that was acceptable at the 90% confidence level, and used this normalization to compute an upper limit to the flux from unresolved point sources.

The surface brightness of the diffuse emission that can be accounted for by unresolved point sources is listed by region in Table 1, and is displayed graphically in Figure 6. Unresolved point sources may produce $(0.7 - 1.5) \times 10^{-13}$ erg cm^{-2} s^{-1} arcmin^{-2} in the regions $7'$ from the Galactic center, which is 35–80% of the total observed diffuse flux. We also list in Table 1 the flux from the soft and hard components that remains when an unresolved point source contribution is included. The reduction in the inferred diffuse flux is most dramatic in the hard band. Nevertheless, including a point source contribution in the Northeast, Northwest, and East does not removed the need for an 8 keV plasma component.

The significant differences between the upper limits to the unresolved point source contribution in each region occur because the fluxes and ratios of the fluxes in the He-like and H-like Fe lines are spatially variable (Figure 6), and they match the spectra of the point sources better in some regions than in others. Since the surface brightness from resolved point sources is relatively constant from field-to-field in the dark regions (Table 1), it seems unlikely that the surface brightness of unresolved point sources at the Galactic center actually varies from field-to-field by a factor of two. It is equally unlikely that the average spectra from hundreds of point sources varies on arcminute scales. Therefore, the most reasonable upper limit to the unresolved flux from point sources is the lowest inferred value: 7×10^{-14} erg cm^{-2} s^{-1} arcmin^{-2} in the Northwest dark region.

We can use this value and the $\log(N) - \log(S)$ distribution from Equation 5 in Muno et al. (2003a) to compute an upper limit to the surface density of unresolved point sources near the Galactic center. We find that the total point-source flux in the Northwest region of Figure 2 could be produced by the integrated flux from sources brighter than $S_{\rm min} = 4 \times 10^{-16}$ erg cm^{-2} s^{-1}. This is only a factor of ten lower than the completeness limit of Muno et al. (2003a), and it corresponds to a luminosity of 3×10^{30} erg s^{-1} at 8 kpc. Moreover, this flux limit implies that there are 95 sources arcmin^{-2} at an offset from Sgr A* of $\theta = 8'$, which is 40 times higher than the number of sources resolved there by Muno et al. (2003a). Since the surface density of point sources increases as θ^{-1} toward Sgr A*, there could be as many as 750 sources arcmin^{-2} within $1'$ of Sgr A*.

4. DISCUSSION

We have shown that unresolved point sources brighter than 3×10^{30} erg s^{-1} can account for nearly half of the hard component of the diffuse emission. Producing this amount of flux in the $17'$ by $17'$ around Sgr A* in Figure 2 would require over 44,000 point sources. The most likely candidates for such a large population of hot ($kT \sim 8$ keV) X-ray sources are cataclysmic variables (CVs;see Eracleous, Halpern, & Patterson 1991; Mukai & Shiokawa 1993; Ezuka & Ishida 1999). Approximately 60% of CVs in the *ROSAT* sample of Verbunt et al. (1997) have luminosities higher than 3×10^{30} erg s^{-1}, so we would infer that unresolved $\sim 7 \times 10^4$ CVs are present near the

Galactic center. This would imply a spatial density of 0.1 pc^{-3} in a volume of $40 \times 40 \times 300$ pc, which is 3000 times higher than the local space density of CVs (Schwope et al. 2002). Such a density of CVs is not unreasonable, since the stellar density within the inner 20 pc of the Galaxy is $\sim$ 6000 times higher than the local value (Launhardt, et al. 2002).

On the other hand, unresolved point sources can not produce all of the hard diffuse emission from the Galactic center, and so its origin is therefore still an open question. The 0.8 keV plasma is probably produced by supernova, which are the largest heating source for the ISM. Indeed, $\sim$ 1 keV plasma is commonly inferred to be present in supernova remnants, and the energy required to heat the plasma is only fraction of the kinetic energy known to be released by supernova. In contrast, supernova rarely produce plasma with $kT \gtrsim 3$ keV (Kaneda et al. 1997). Therefore, the hard diffuse emission has been variously modeled as originating from plasma heated and confined by magnetic filaments (Tanuma et al. 1999), quasi-thermal plasma continuously accelerated by shocks in the 0.8 keV plasma (Dogiel et al. 2002; Masai et al. 2002), and emission from cosmic-ray electrons (Valinia et al. 2000). These mechanisms are not entirely satisfying yet, because they all require significant assumptions about processes for which we have few other observational constraints (see the discussion in, e.g., Dogiel et al. 2002).

Further progress in understanding the origin of the diffuse X-ray emission from the Galactic plane awaits observations with much higher energy resolution. The major predictions of the quasi-thermal plasma and cosmic-ray models are that the line strengths and ratios in the diffuse emission should differ significantly from their collisional-equilibrium values (Valinia et al. 2000; Masai et al. 2002). Unfortunately, the current *Chandra* observations appear unable to distinguish these from variations in the elemental abundances. ASTRO-E 2 will have a factor of 10 better energy resolution than ACIS-I on *Chandra*, which will enable us to resolve the He-like $n = 2 - 1$ triplet from Fe, and to detect radiative recombination continua from Si, S, Ar, and Fe. Therefore, the prospects for understanding the source of the hard diffuse X-ray emission within the next decade are excellent.

First, I would like to thank Fred Baganoff for bringing me onto this project right after I finished my Ph.D. I am also grateful to all of my collaborators on these Galactic center observations, for their advice on scientific issues, help with software, and insistence that I remain honest. Those collaborators are: Fred Baganoff, Mark Bautz, Niel Brandt, Pat Broos, Eric Feigelson, Gordon Garmire, Christian Howard, Mark Morris, Sangwook Park, George Ricker, and Leisa Townsley. This work was supported in part by NASA grants NAS 8-39073 and NAS 8-00128, and by a Hubble Fellowship grant from the Space Telescope Science Institute, which is operated by the Association of Universities for Research in Astronomy, Incorportated, under NASA contract NAS5-26555.

REFERENCES

Baganoff, F. K. et al. 2003, ApJ, 591, 891
Bamba, A., Ueno, M., Koyama, K., & Yamauchi, S. 2003, ApJ, 583, 253
Dogiel, V. A., Inoue, H., Masai, K., Schönfelder, V., & Strong, A. W., 2002, ApJ, 581, 1061
Ebisawa, K., Maeda, Y., Kaneda, H., & Yamauchi, S. 2001, Science, 293, 1633
Eracleous, M., Halpern, J., & Patterson, J. 1991, ApJ, 382, 290
Ezuka, H. & Ishida, M. 1999, ApJS, 120, 277
Kaneda, H., Makishima, K., Yamauchi, S., Koyama, K., Matsuzaki, K., & Yamasaki, N. Y. 1997, ApJ, 491, 638
Koyama, K., Maeda, Y., Sonobe, T., Takeshima, T., Tanaka, Y., & Yamauchi, S. 1996, PASJ, 48, 249
Lu, F. J., Wang, Q. D., & Lang, C. C. 2003, AJ, 126, 319
Launhardt, R., Zylka, R., & Mezger, P. G. 2002, A&A, 384, 112
Masai, K., Dogiel, V. A., Inoue, H., Schönfelder, V., & Strong, A. W., 2002, ApJ, 581, 1071
Mukai, K. & Shiokawa, K. 1993, ApJ, 418, 863
Muno, M. P., Baganoff, F. K., Bautz, M. W., Brandt, W. N., Broos, P. S., Feigelson, E. D., Garmire, G. P., Morris, M., Ricker, G. R., & Townsely, L. K. 2003a, ApJ, 589, 225
Murakami, H., Koyama, K., Sakano, M., & Tsujimoto, M. 2000, ApJ, 534, 283
Park, S., Baganoff, F. K., Morris, M., Maeda, Y., Muno, M. P., Howard, C., Bautz, M. W., & Garmire, G. P. 2003, submitted to ApJ
Sakano, M., Warwick, R. S., Decourchelle, A., & Predehl, P. 2003, MNRAS, 340, 747
Schwope, A. D., Brunner, H., Buckley, D., Greiner, J., Heyden, K. v. d., Neizvestny, S., Potter, S., & Schwarz, R. 2002, A&A, 396, 895
Sunyaev, R., Markevitch, M., & Pavlinsky, M. 1993, ApJ, 407, 606
Tanuma, S., Yokoyama, T., Kudoh, T., Matsumoto, R., Shibata, K., & Makishima, K. 1999, PASJ, 51, 161
Valinia, A., Tatischeff, V., Arnaud, K., Ebisawa, K., & Ramaty, R. 2000, ApJ, 435, 733
Verbunt, F., Bunk, W. H., Ritter, H., & Pfeffermann, E. 1997, A&A, 327, 602
Wang, Q. D., Gotthelf, E. V., & Lang, C. C. 2002, Nature, 415, 148
Weisskopf, M. C., Brinkman, B., Canizares, C., Garmire, G., Murray, S., van Speybroeck, L. P. 2002, PASP, 114, 1
Yamauchi, S., Kaneda, H., Koyama, K., Makishima, K., Matsuzaki, K., Sonobe, T., Tanaka, Y., & Yamasaki, N. 1996, PASJ, 48, L15
Yusef-Zadeh, F., Law, C., & Wardle, M. 2002, ApJ, 568, L125

TABLE 1
FLUX FROM THE PLASMA COMPONENTS AND POINT SOURCES

	Southeast	Southwest	Northwest	East	Close	Northeast
$F_{\rm tot}$	1.80	1.84	1.72	2.27	3.02	4.49
$F_{\rm resolved}$	0.2	0.3	0.2	0.2	1.0	X
No Unresolved Point Sources						
F_1	0.26	0.17	0.20	0.62	0.36	1.83
F_2	1.47	1.64	1.53	1.63	2.48	2.64
With Unresolved Point Sources						
F_1	0.49	0.02	0.23	0.52	0.54	1.68
F_2	0.04	0.37	0.81	0.91	0.06	1.93
$F_{\rm unresolved}$	1.27	1.46	0.68	0.84	2.42	0.87

Note. — All fluxes are those observed between 2–8 keV, in units of 10^{-13} erg cm^{-2} s^{-1} arcmin^{-2}.

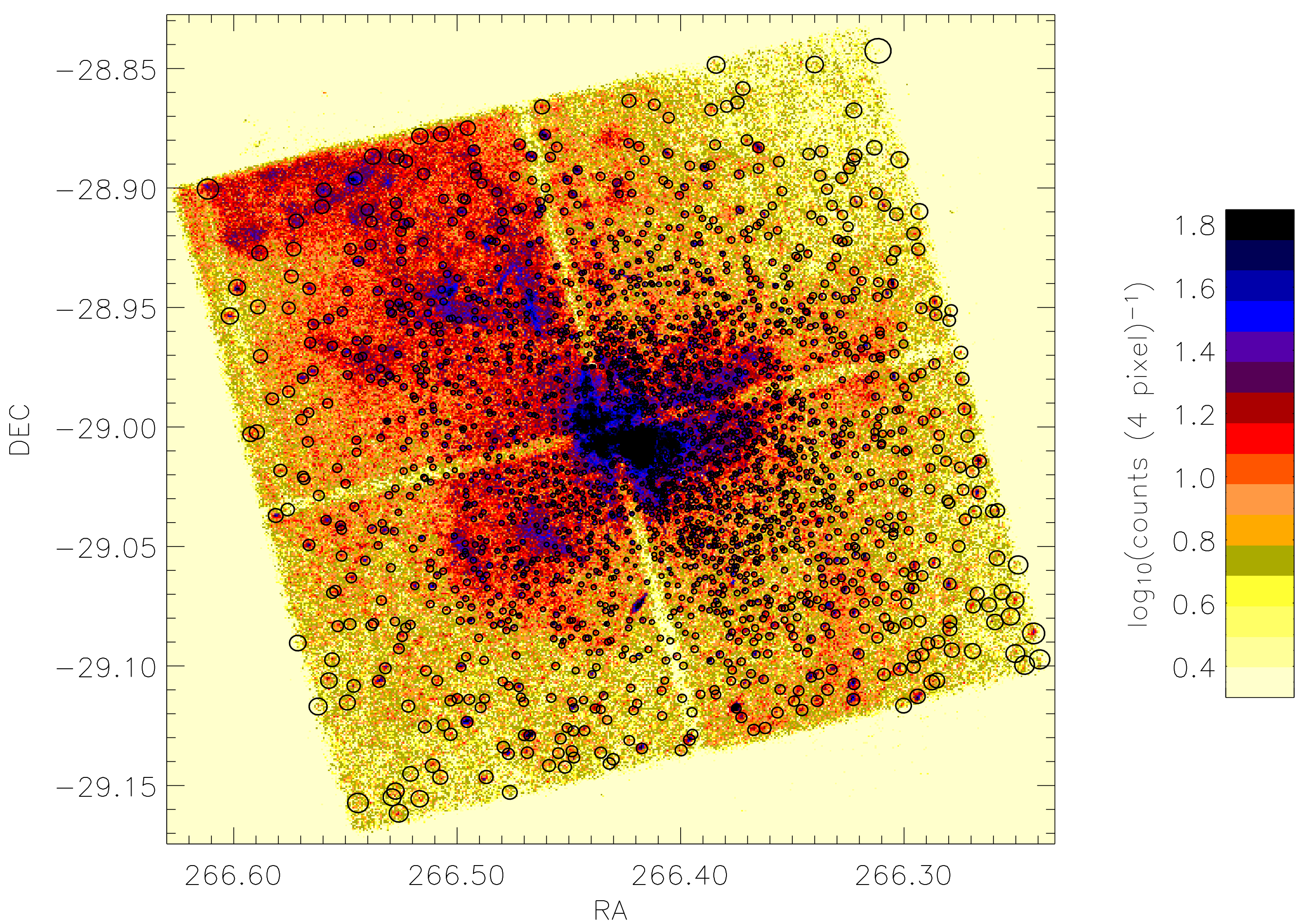

FIG. 1.— Raw image of counts received in the Sgr A* field. The image has been binned to have 2″ pixels. The circles that were used to exclude the 2353 point sources detected by Muno et al. (2003a) have been overlaid on the image. The Sgr A complex is saturated in the center of the image. Also evident are bipolar lobes centered on Sgr A* and oriented perpendicular to the Galactic plane, hard filamentary features to the northeast and south of the Sgr A complex, and bright, diffuse emission throughout the image (see Baganoff et al. 2003; Park et al. 2003).

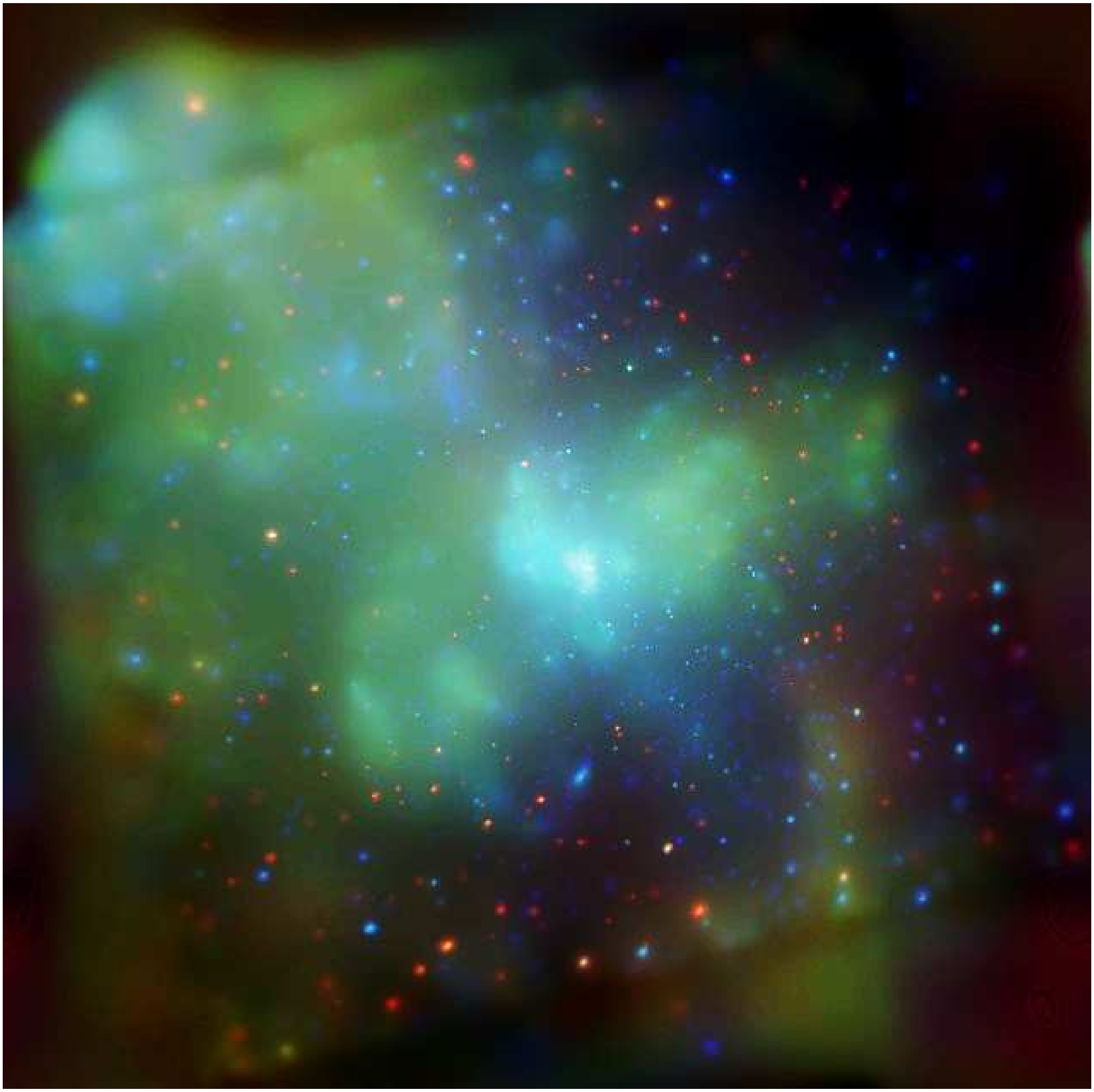

FIG. 2.— Three-color, smoothed image of the Sgr A* field. The red band is made from photons between 0.5–2.0 keV, the green from 2.0–4.0 keV, and the blue from 4.0–8.0 keV. The red sources lie in the foregound, and were not included in the analysis in this paper. Otherwise, the bulk of the diffuse emission is observed from the Galactic center between 2–8 keV. The point sources located near the Galactic center are most prominent in the 4–8 keV band.

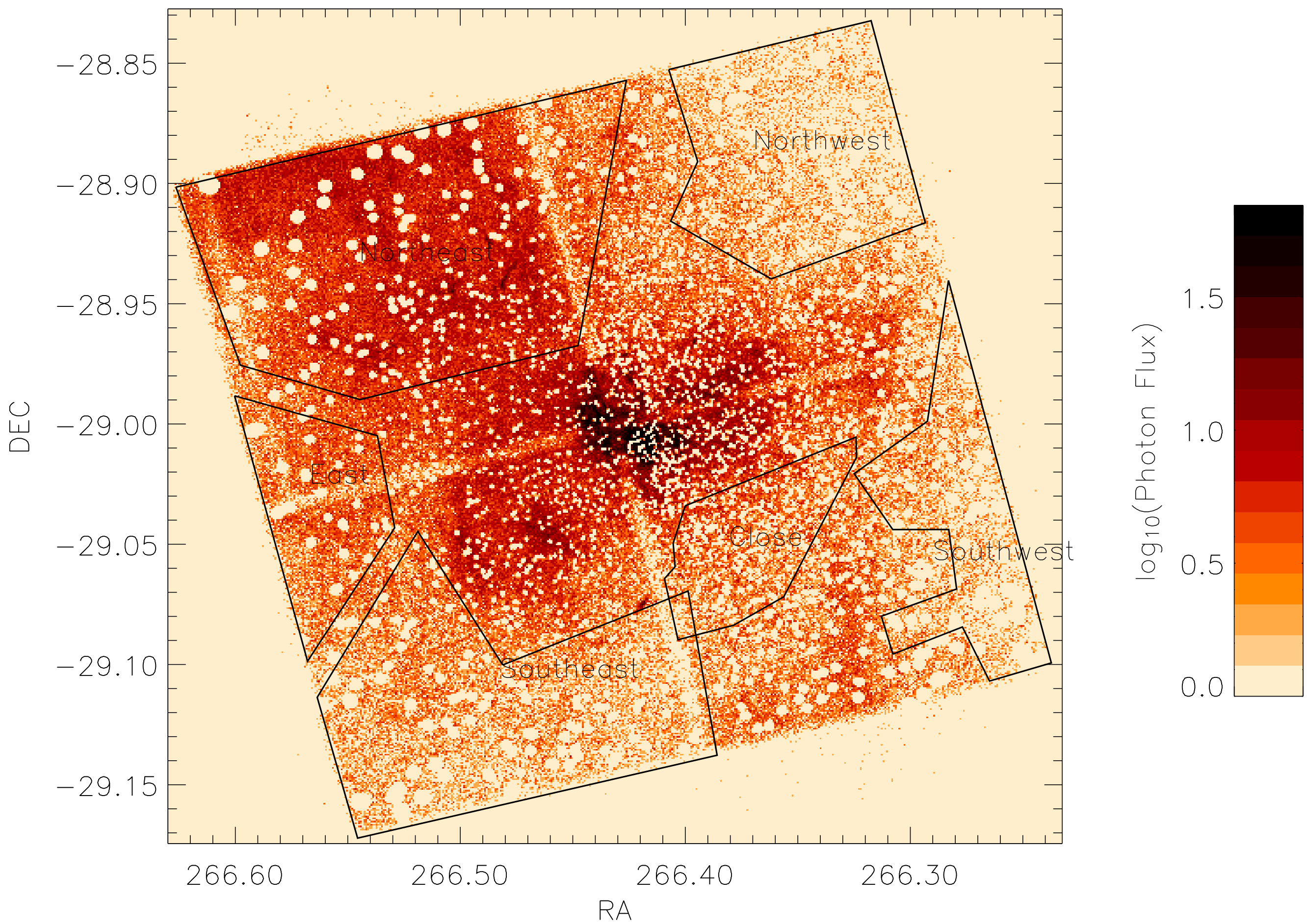

FIG. 3.— Image of the Sgr A* field in the 2–4 keV band, overlaid with the polygonal regions from which the spectra of the diffuse emission were extracted. The soft emission is most prominent at the bipolar lobes centered on Sgr A*, in the northeast, and in a ridge of emission in the Southwest.

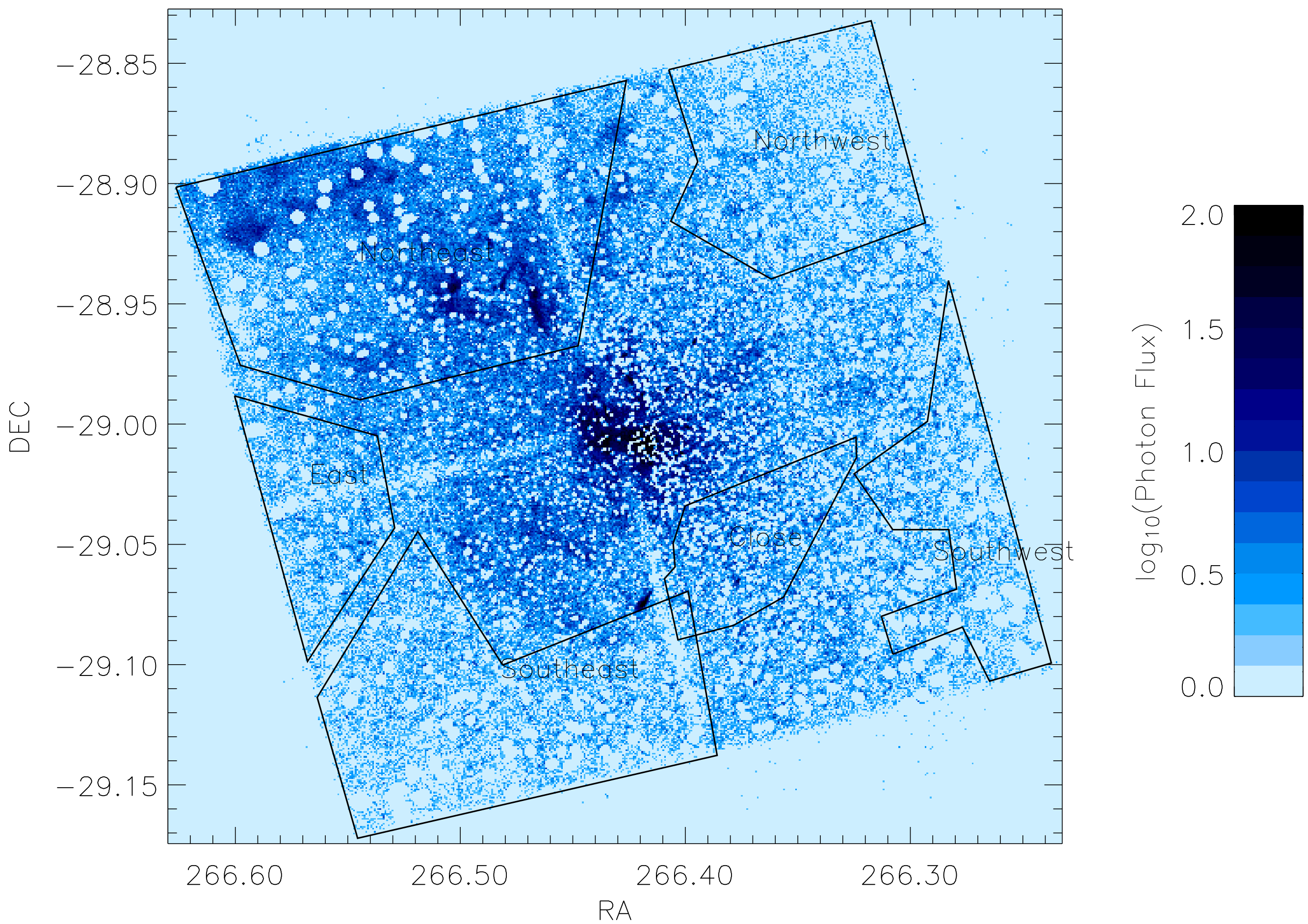

FIG. 4.— Image of the Sgr A* field in the 4–8 keV band, overlaid with the polygonal regions from which the spectra of the diffuse emission were extracted. The hard emission is more uniformly distributed in the soft, but is somewhat stronger in the northeast, particularly at several compact sites of neutral Fe emission (Park et al. 2003).

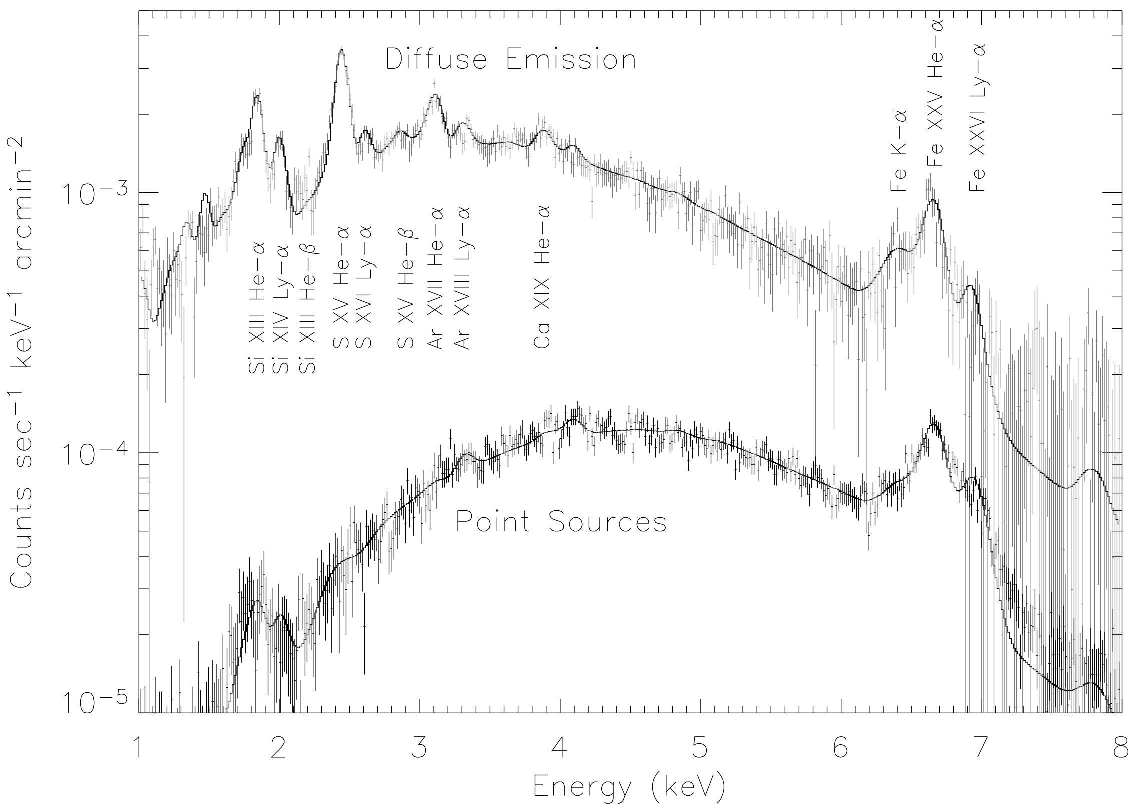

FIG. 5.— A comparison between the spectra of the point sources and diffuse emission from the Southeast region near the Galactic center. The relative normalizations of the two spectra accurately reflect their relative fluxes — the flux from point sources is about 10% of that from the diffuse emission. The average spectrum of the point sources is considerably harder than that of the diffuse emission. The identifications of the prominent emission lines are also indicated.

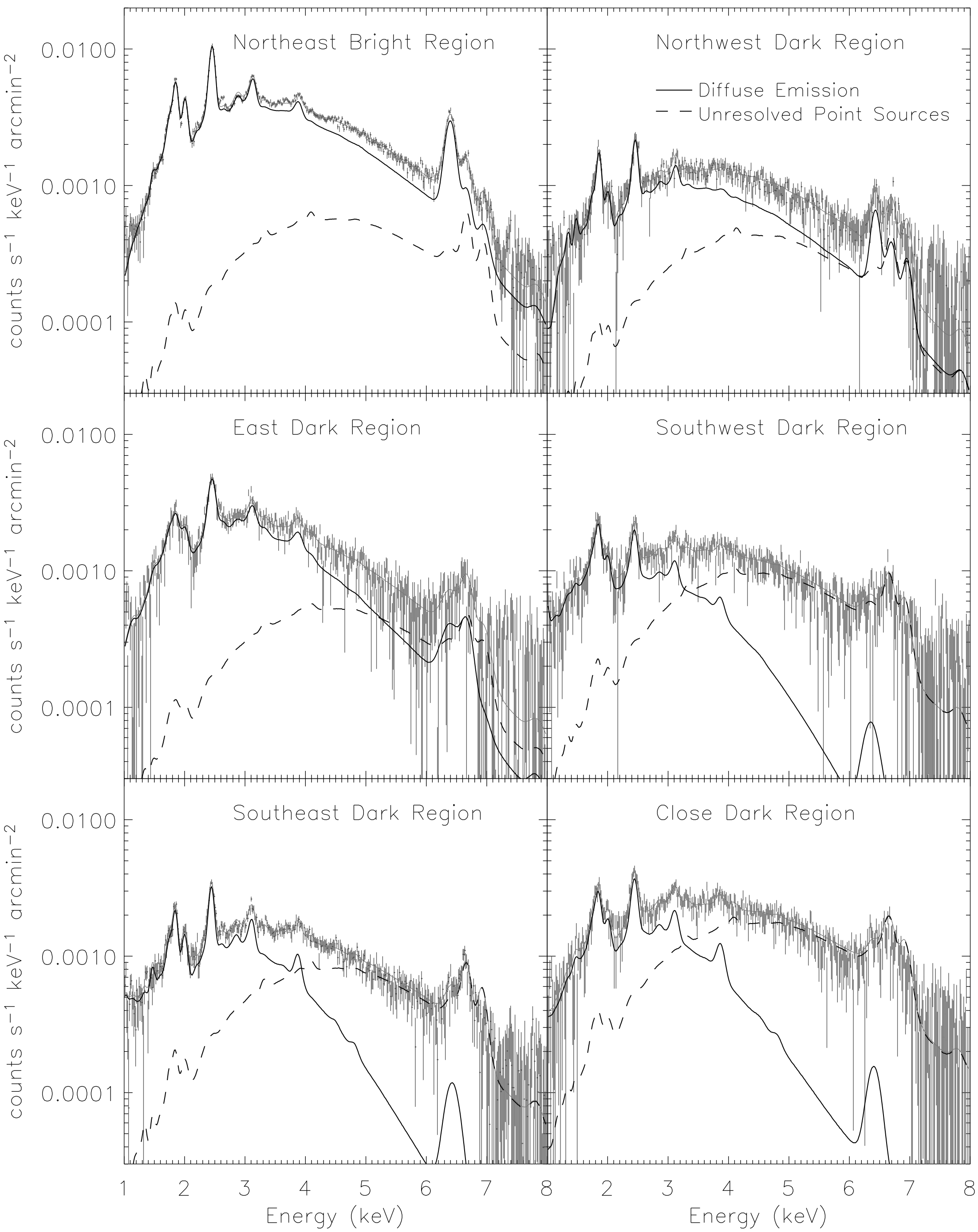

FIG. 6.— This figure illustrates the maximum amount that unresolved point sources could plausibly contribute to the diffuse emission. The background-subtracted spectrum of the diffuse emission is shown with the grey crosses. The upper limit to the contribution of unresolved point sources is based upon the spectrum of resolved sources with fewer than 80 net counts, and is shown with the dashed line. The remaining emission inferred to be truly diffuse is shown with the solid black line. The point sources are much harder than the total diffuse emission, but can not be responsible for all of the inferred hard component of the diffuse emission.